AGU PUBLICATIONS

JGR

Journal of Geophysical Research: Atmospheres

RESEARCH ARTICLE

10.1002/2015JD023602

Key Points:

- Terra band 29 has strong crosstalk effect
- Crosstalk correction algorithm is applied to correct the crosstalk effect
- The crosstalk effect is significantly reduced with the correction algorithm

Correspondence to:
J. Sun,
junqiang.sun@noaa.gov

Citation:
Sun, J., S. Madhavan, X. Xiong, and M. Wang (2015), Long-term drift induced by the electronic crosstalk in Terra MODIS Band 29, *J. Geophys. Res. Atmos.*, *120*, 9944–9954, doi:10.1002/2015JD023602.

Received 30 APR 2015
Accepted 9 SEP 2015
Accepted article online 14 SEP 2015
Published online 5 OCT 2015

Long-term drift induced by the electronic crosstalk in Terra MODIS Band 29

Junqiang Sun[1,2], Sriharsha Madhavan[3], Xiaoxiong Xiong[4], and Menghua Wang[1]

[1]NOAA National Environmental Satellite, Data, and Information Service, Center for Satellite Applications and Research, College Park, Maryland, USA, [2]Global Science and Technology, Greenbelt, Maryland, USA, [3]Science Systems and Applications Inc., Lanham, Maryland, USA, [4]Sciences and Exploration Directorate, NASA/GSFC, Greenbelt, Maryland, USA

Abstract Terra MODerate Resolution Imaging Spectroradiometer (MODIS) is one of the key sensors in the NASA's Earth Observing System, which has successfully completed 15 years of on-orbit operation. Terra MODIS continues to collect valuable information of the Earth's energy radiation from visible to thermal infrared wavelengths. The instrument has been well characterized over its lifetime using onboard calibrators whose calibration references are traceable to the National Institute of Standards and Technology standards. In this paper, we focus on the electronic crosstalk effect of Terra MODIS band 29, a thermal emissive band (TEB) whose center wavelength is 8.55 μm. Previous works have established the mechanism to describe the effect of the electronic crosstalk in the TEB channels of Terra MODIS. This work utilizes the established methodology to apply to band 29. The electronic crosstalk is identified and characterized using the regularly scheduled lunar observations. The moon being a near-pulse-like source allowed easy detection of extraneous signals around the actual Moon surface. First, the crosstalk-transmitting bands are identified along with their amplitudes. The crosstalk effect then is characterized using a moving average mechanism that allows a high fidelity of the magnitude to be corrected. The lunar-based analysis unambiguously shows that the crosstalk contamination is becoming more severe in recent years and should be corrected in order to maintain calibration quality for the affected spectral bands. Finally, two radiometrically well-characterized sites, Pacific Ocean and Libya 1 desert, are used to assess the impact of crosstalk effect. It is shown that the crosstalk contamination induces a long-term upward drift of 1.5 K in band 29 brightness temperature of MODIS Collection 6 L1B, which could significantly impact the science products. The crosstalk effect also induces strong detector-to-detector differences, which result in severe stripping in the Earth view images. With crosstalk correction applied, both the long-term drift and detector differences are significantly reduced.

1. Introduction

Terra MODerate Resolution Imaging Spectroradiometer (MODIS) is a premier sensor in the network of NASA's Earth Observing System and continues to collect high-quality remotely sensed information of the Earth in solar reflective and thermal infrared wavelengths, and is well past its design lifetime of 6 years [*Salomonson et al.*, 2002; *Barnes et al.*, 2002]. Launched on 18 December 1999, Terra MODIS has completed its 15 year anniversary, with the derived science data products contributing immensely to the understanding of Earth sciences [*Xiong et al.*, 2007, 2008]. The 16 Thermal Emissive Bands (TEB) have been well regarded to be stable in their performance [*Xiong et al.*, 2009; *Wenny et al.*, 2013]. However, recent works have examined and established the crosstalk leaks, which induce strong striping, ghost image, as well as long-term drifts to be as significant as 6 K and 3 K effect in Earth View (EV) Brightness Temperature (BT) for bands 27 and 28, respectively, over the past 15 years [*Sun et al.*, 2011, 2014a, 2014b, 2014c; *Madhavan et al.*, 2014]. Recent vicarious ground and inter sensor comparisons with ASTER have shown that Terra MODIS band 29 has a temporal bias in measurements around the typical radiance levels [*Hook et al.*, 2014]. Following up on the previous crosstalk work in Terra bands 27 and 28, it became imperative to investigate the crosstalk effect and to study the impact and correction of electronic crosstalk in band 29.

MODIS band 29 is a surface-sensing thermal channel and is predominantly used for understanding cloud properties. Over the mission of Terra MODIS, the performance of band 29 is deemed as stable with the exception of its detector 6 (product order). It was found that the noise level of band 28 detector 6 had a significant jump in 2005 such that its Noise Equivalent differential Temperature (NEdT) became at least 4 times the noise specification for this band. Since 2005 this detector has been classified as inoperable in MODIS Level 1B (L1B)

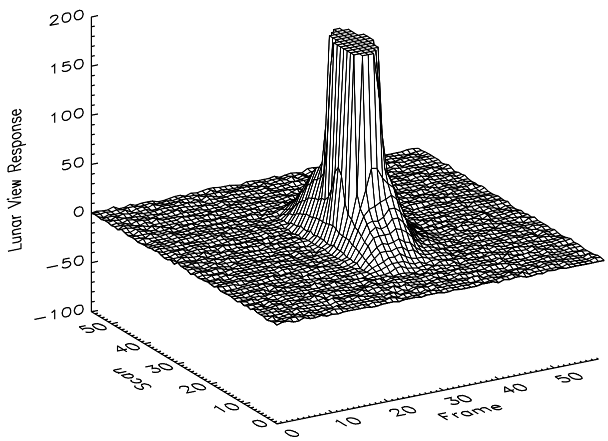

Figure 1. Lunar image of Terra band 29 detector 6 on 21 June 2000.

products. The rest of the detectors operate nominally and are within the required NEdT specifications for this band, but clear increases of the NEdT are seen recently [*Xiong et al*., 2008]. In this paper, it will be shown that the NEdT jump is sourced to the crosstalk effect and that the band is significantly affected by electronic crosstalk, with detector 6 in product order being the worst affected although the band seems stable in performance. In addition, the on-orbit long-term performances have indicated large long-term drifts in the instrument gain for all the photovoltaic (PV) long-wave infrared (LWIR) bands. Bands 27 and 30 have large percentage drifts since 2003 at about −15.6% and −15.2%, respectively. Bands 28 and 29 have changed by about −10.3% and −12.4%, respectively [*Xiong et al*., 2015]. In comparison, all other TEBs have long-term changes within 2.5%. Such long-term drifts are indeed a cause for concern as a systematic drift is also observed in the retrieved Earth View (EV) radiances. Recently reported by the MODIS science user community, several of the cloud detection schemes that use these affected bands have been impacted, due to these long-term degradations in response. The crosstalk effect may bring a long-term drift in the EV BT of L1B products as demonstrated in the EV BT of Terra bands 27 and 28. It will be shown that the crosstalk effect indeed induced a long-term upward drift of 1.5 K in the EV BT, which is different from those in bands 27 and 28 where the drifts are downward. It will also be shown that the crosstalk effect induces jumps in the calibration coefficients derived from the black body (BB) calibration and strong detector differences which result in heavy striping in the EV images.

In this paper, we characterize the crosstalk effect for Terra band 29 using the scheduled lunar observations [*Sun et al*., 2007; *Sun and Xiong*, 2011] and apply the crosstalk correction algorithms we recently developed to remove the crosstalk effect in both calibration coefficients and EV L1B products. In this analysis, MODIS most recent version, Collection 6 (C6), of L1B products is used as the EV products before crosstalk correction [*Wenny et al*., 2012]. Thus, keeping the above objectives in mind, the paper is organized as follows. The next section details the crosstalk phenomenon and its characterization using the regular moon observations from the Space View (SV) port. Section 3 discusses the improvements seen in the Black Body (BB) calibration after electronic crosstalk correction for Terra band 29. Section 4 will show the EV image quality improvements with crosstalk correction. It will also show the long-term drift induced by the crosstalk in the band's EV BT and its removal with the crosstalk correction. Finally, the paper is closed with a summary of the work and future effort.

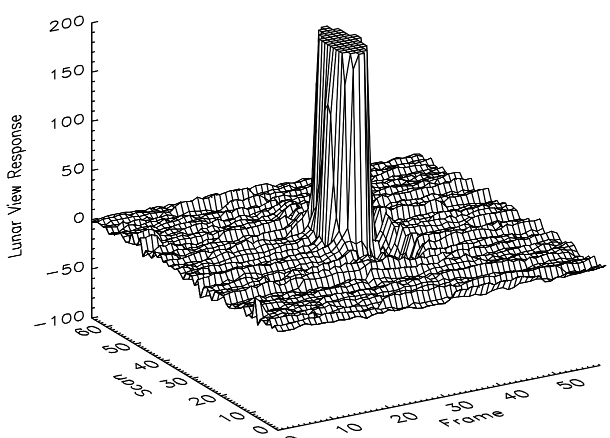

Figure 2. Lunar image of Terra band 29 detector 6 on 8 June 2012.

2. Crosstalk Phenomenon and Coefficients

For the assessment on the level of crosstalk contamination the Moon surface is an ideal target [*Li et al*., 2005; *Sun et al*., 2011, 2014a]. Figures 1 and 2 are two sets of lunar observations for band 29 detector 6 presented in the form of a three-dimensional surface plot. The Moon acquisitions shown are obtained on 21 June 2000 and the other on 8 June 2012, respectively. The along-track direction of the spacecraft is denoted as the scan direction, and the across-track swath is referred to as frame direction. The *x* and *y* axes represent the frames and scans,

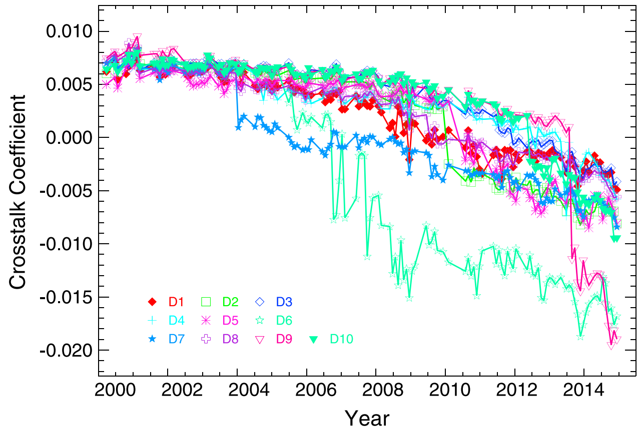

Figure 3. Terra band 29 crosstalk coefficients for sending band 27.

and the *z* axis gives the actual Moon digital response. The lunar size for each of the 1 km bands is about 7 × 7 pixels. Due to oversampling effect [*Sun et al.*, 2011], there are several scans corresponding to one pixel in the along-track direction and thus, there is an elongation effect in the lunar images shown in Figures 1 and 2. The oversampling factor is event dependent, and thus, the elongation effect varies with events. For illustration purposes and to identify the crosstalk magnitude, the Moon signal is truncated to within 200 digital numbers (DN). The maximal response can be as high as 4000 DN. In fact, Terra band 29 as well as bands 27–30 all saturate when they view in the center part of the Moon. However, band 31 does not saturate for an entire lunar image. With an assumption that there is a linear relationship between DNs of any of bands 27–30 and those of band 31, the DNs of the band in the saturated area can be estimated from the DNs of band 31 and the ratios of the two bands' DNs in the unsaturated region [*Sun et al.*, 2014a]. From Figure 1, a tiny protrusive feature is observed near the bottom of the oval cylindrical structure. A clean Moon signal would produce an oval cylindrical structure with sharp boundary surface illustrating the lunar surface against the dark space background. Thus, the tiny protrusive feature demonstrates that there is crosstalk effect in Terra band 29. From Figure 1, it is also seen that the crosstalk contribution to the instrument response of band 29 detector 6 is positive on 21 June 2000. In Figure 2, the bottom surrounding area becomes negative; this indicates that there is crosstalk contamination, and the crosstalk contribution for Terra band 29 detector 6 is negative on 8 June 2012. This demonstrates that the crosstalk effect for Terra band 29 changes with time, same as that for Terra bands 27 and 28 [*Sun et al.*, 2011, 2014a, 2014b, 2014c, 2015; *Madhavan et al.*, 2014]. As demonstrated in Figures 1 and 2, the cause of the crosstalk effect is not optical but somehow electronic. However, the exact nature of the electronic effect is not yet well enough understood to allow us to develop and apply any physical sensor model to describe and correct for these effects, even though a linear algorithm has developed to describe the crosstalk effect and the algorithm works pretty well [*Sun et al.*, 2014a, 2014b, 2015].

For a MODIS TEB, the crosstalk contribution from other bands can be approximated by the expression [*Sun et al.*, 2011, 2014a]

$$\mathrm{d}n_{B,D_r}^{\mathrm{xtalk}}(F) = \sum_{B_s} C(B_r, D_r, B_s) \left\langle \mathrm{d}n_{B_sD_s}^{\mathrm{msr}}(F + \Delta F_{\mathrm{rs}}) \right\rangle_{D_s}, \quad (1)$$

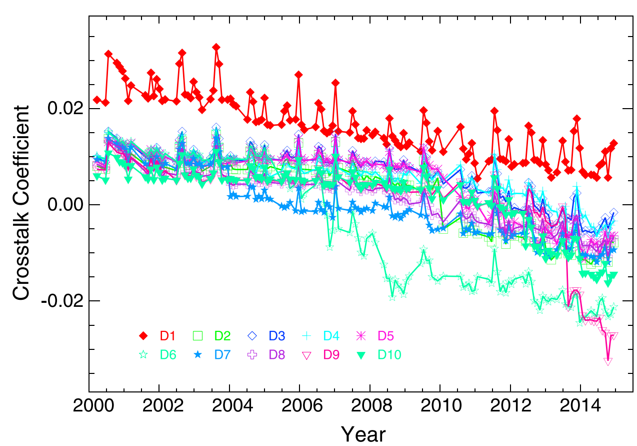

Figure 4. Terra band 29 crosstalk coefficients for sending band 28.

where B_r is the receiving band, D_r is the receiving detector, B_s is the sending band, D_s is the sending detector, $C(B_r,D_r,B_s)$ is the effective crosstalk coefficient from band B_s to band B_r and detector D_r, F is the frame number (pixel number along scan) of B_r, ΔF_{rs} is the frame shift between band B_r and band B_s for viewing the same target, $\mathrm{d}n_{B_sD_s}^{\mathrm{msr}}(F + \Delta F_{\mathrm{rs}})$ is the background-subtracted measured instrument response of band B_s, detector D_s at frame $F + \Delta F_{\mathrm{rs}}$, and finally the brackets indicate the average over the detectors of band B_s. The instrument response uncontaminated by the crosstalk effect is derived by removing the correction value from the measured response. As shown in Figures 1 and 2, the

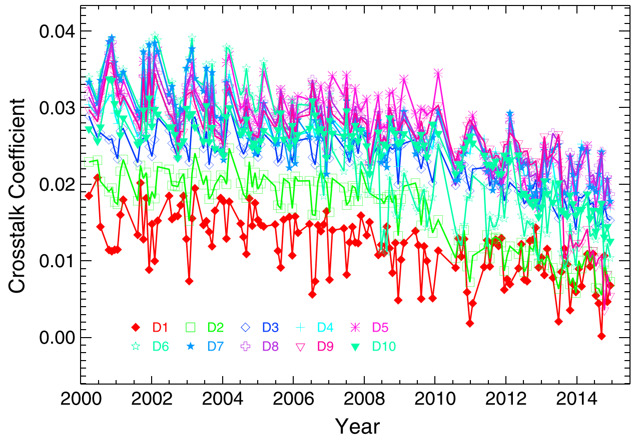

Figure 5. Terra band 29 crosstalk coefficients for sending band 30.

artifacts of the crosstalk effect can be best observed in lunar measurements due to the "knife edge" nature of the lunar observations and then the lunar measurements can be used to derive the effective crosstalk coefficient, $C(B_r,D_r,B_s)$ [*Sun et al.*, 2014a], which are important and useful for the crosstalk effect removal. The frame shift ΔF_{rs} for receiving band B_r and sending band B_s is a constant, which is the case for Terra MODIS TEB [*Xiong et al.*, 2006]. If it is an integer or it changes with time due to change of the band to band registration, equation (1) needs to be slightly modified. It is also worth to mention that a linear relationship between the crosstalk contribution of a send band and its background-subtracted instrument response is applied in equation (1) but the nature of the crosstalk effect may not, in principle, necessarily be linear. However, the linear approximation works pretty well as demonstrated in Terra bands 27 and 28 [*Sun et al.*, 2014a, 2014b, 2015] and also later sections.

The crosstalk characterization based on the lifetime moon observations is shown in Figures 3–5. The characterization is based on a linear model shown in equation (1). The effective crosstalk coefficient from each sending band is calculated as a band-averaged estimate and modeled for each detector on the receiving band. Figure 3 gives the crosstalk coefficient magnitude for sending band 27. All detectors in band 29 start out having a positive contribution of magnitude close to 0.007 and then a trending in the negative direction over time with different amounts at varying times for each of the detectors. Two detectors stand out in terms of their long-term changes. Detectors 6 and 9 seem to be the most affected, with detector 6 being severely affected since late 2005, and detector 9 just recently. The magnitude change is as high as about −0.023 for both detectors by the end of 2014. The rest of the detectors have also exhibited a significant drift to about −0.015 by 2014. Figure 4 gives the crosstalk magnitude amount for sending band 28. It is worth to draw attention that there are observable seasonal oscillations in the effective crosstalk coefficients shown in Figures 3–5. It may suggest that crosstalk effects are not static and the effective crosstalk correction coefficients are not stable over time frames of many months. However, variations of the crosstalk coefficients could be induced by the uncertainty of the approach used to derive the coefficients from the lunar observations and may have relationship with the lunar observation view geometry. Investigation of the relationship is beyond the scope of this paper. To minimize the uncertainty due to the seasonal oscillations in the effective crosstalk coefficients, an annually running average of the coefficients is used when the coefficients are applied in the crosstalk correction. If there is a jump in the coefficients, the average is applied separately for the time periods before and after the jump.

In comparison to band 27 the crosstalk magnitude is slightly larger partly owing to its proximity to band 29 on the LWIR focal plane. A slow downward drift is observed in the trending for all detectors with the exception of detectors 6 and 9. Another slight exception is detector 1 whose coefficients have trended to be positive throughout the lifetime. The crosstalk coefficient for most of the other detectors currently is around −0.008, with the largest change observed for detectors 6 and 9 whose coefficients are close to −0.023 in 2014. Continuing to Figure 5, which gives the crosstalk coefficients from sending band 30, it is noted that the crosstalk magnitude is overall positive throughout the lifetime. Detectors 1 and 2 seem to be the least

Table 1. Crosstalk Effect Comparison Among Bands 27, 28, and 29 in 2012

Band	Absolute Maximum Crosstalk Coefficient 27	28	29	30	Striping at Pacific Ocean (k)	Long-Term Drift at Pacific Ocean (K)
27		0.05	0.065	0.02	10	−6
28	0.025		0.065		3	−1.6
29	0.012	0.02		0.025	1.3	1.1

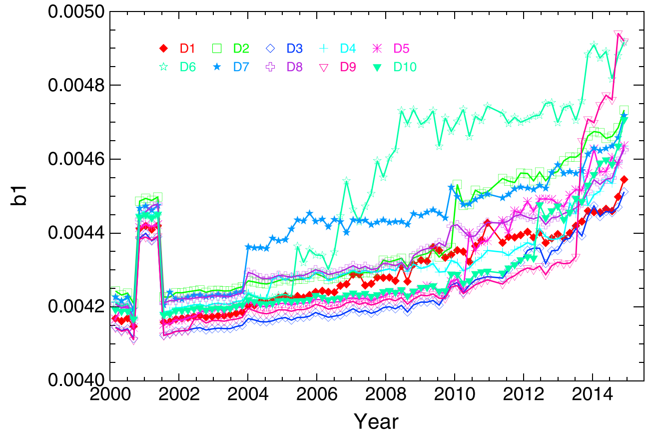

Figure 6. Terra band 29 b_1 before correction for individual detectors.

affected by crosstalk from band 30 as their magnitudes are considerably smaller in comparison to the rest of the detectors. For comparison among bands 27–29 for the crosstalk effect, the maximum crosstalk coefficients among those of the 10 detectors in 2012 for a receiving band from each sending band are listed in columns 2–5 of Table 1. An overall assessment of the coefficients for the receiving band 29 indicates the electronic crosstalk correction to be considerably smaller in comparison to the crosstalk receiving bands 27 and 28 [*Sun et al.*, 2014a] but still to be easily observable.

3. Crosstalk Correction in Black Body Calibration

The TEBs are calibrated on a scan by scan basis using an onboard BB measurement as mentioned earlier [*Xiong et al.*, 2008, 2009]. The calibration is based on a two point source namely the BB and the SV responses. Further, the TEB calibration is based on a quadratic model that converts the digital response to its at sensor aperture radiance. Thermal contributions from scan mirror and cavity are accounted in the model. The linear calibration term often referred to as b_1 is the dominant term of the quadratic equation which accounts for most of the calibration impact. In this paper, we focus on the impact of crosstalk effect on the b_1 coefficients. To remove the crosstalk effect in the calibration coefficients, we need to exclude the crosstalk contribution expressed in equation (1) from the measured BB view instrument response and then calculate the coefficients using the corrected instrument response.

The C6 b_1 coefficients before the crosstalk correction applied for Terra band 6 are displayed in Figure 6. There are sudden jumps in the coefficients of all detectors. Each sudden jump in the coefficients can be connected to a sudden change of the crosstalk coefficients in Figures 3–5. The mechanism for the sudden changes of the crosstalk effect is not known yet. But they should be electronic effect of circuits in the LWIR focal plane assembly. Among all detectors, the b_1 coefficients of detectors 6 and 9 have changed most. This is consistent with the degree of crosstalk contamination demonstrated by the crosstalk coefficients shown in Figure 3–5. The b_1 coefficients of all detectors increase faster in last few years, especially in 2014, which also is consistent with the fact that the crosstalk coefficients of all detectors change faster recently. The b_1 coefficients after the crosstalk correction applied for Terra band 6 are shown in Figure 7. Compared to those in Figure 6, the sudden jumps in Figure 7 are significantly smaller and the changes of the calibration coefficients in the last few years are remarkably reduced. It is also noticeable that the b_1 detector difference becomes smaller after the crosstalk correction. It indicates that the b_1 for all detectors seem to get equalized to an extent that the mismatch in terms of gain is reduced with crosstalk correction. It is also noted that there are some residual b_1 differences which are characteristics of individual detectors which are directly related to the differences of the photoemission efficiencies of the individual detectors and differences of their electronic signal amplifications.

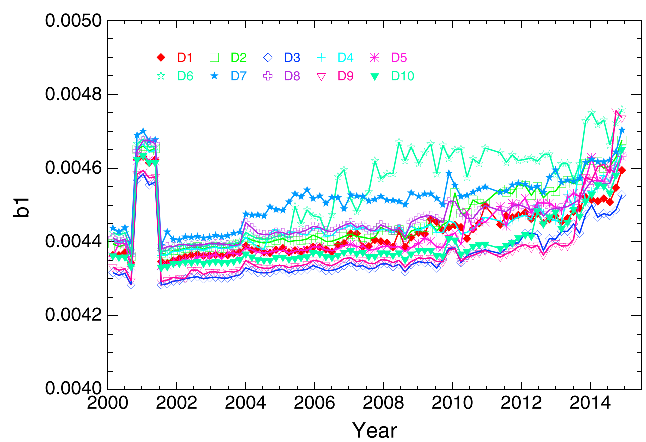

Figure 7. Terra band 29 b_1 after correction for individual detectors.

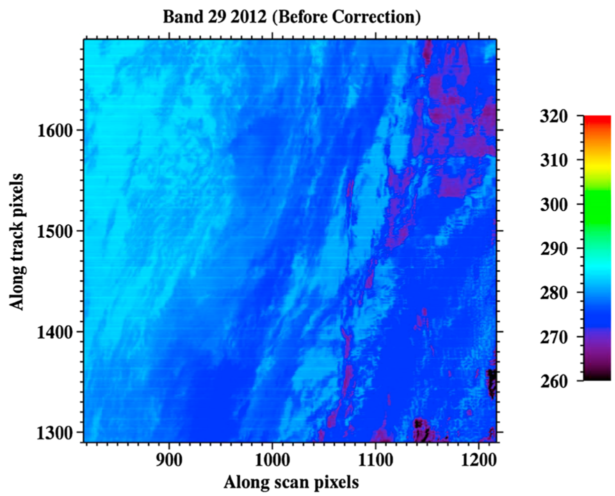

Figure 8. Terra MODIS band 29 C6 EV BT at Baja area before crosstalk correction.

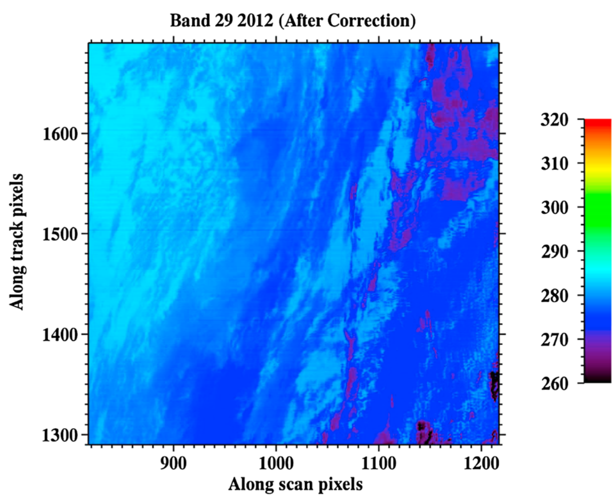

Figure 9. Terra MODIS band 29 C6 EV BT at Baja area after crosstalk correction.

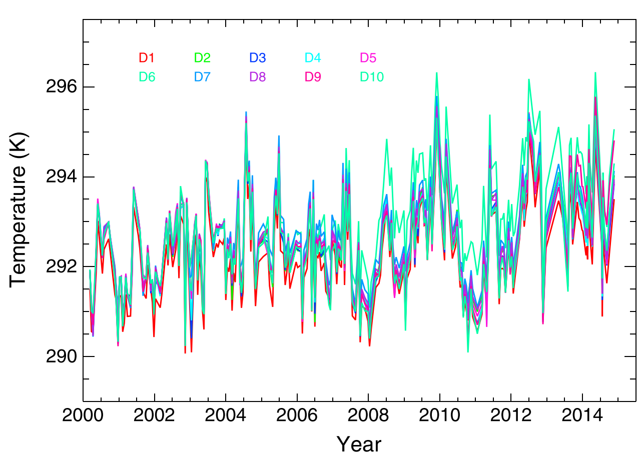

Figure 10. Terra MODIS band 29 C6 brightness temperature at Pacific Ocean.

4. Crosstalk Impact on L1B EV Products

The crosstalk may induce striping due to the detector dependence of the crosstalk effect [*Sun et al.*, 2014a, 2015]. For Terra band 29, the crosstalk effect indeed varies with the detector as demonstrated by the crosstalk coefficients in Figures 3–5. Figure 8 shows a C6 EV image observed in 2012 before the crosstalk correction at Baja area. As expected, the striping is clearly seen in the image. Figure 9 shows the image after the crosstalk correction. The striping is indeed significantly reduced. This indicates that the striping is mainly induced by the crosstalk effect, and the crosstalk correction algorithm described in equation (1) works pretty well.

The crosstalk may induce a long-term drift if the crosstalk effect changes with time besides the striping. The long-term drift is also strongly detector dependent as demonstrated in bands 27 and 28 [*Sun et al.*, 2014b, 2015]. In order to quantify the nature of improvements seen in terms of the long-term drift for band 29, a radiometric analysis is performed using two well-characterized test sites- Libya 1 desert and the Pacific Ocean. These sites have proven to be good benchmark test sites from the earlier works reported in *Sun et al.* [2014b, 2015].

The Pacific Ocean site is a fairly well-understood site as an EV target for thermal channels and generally provides signal levels close to the typical temperatures for most MODIS TEB including band 29. Figure 10 shows the lifetime Terra MODIS band 29 BT trend of the Pacific Ocean site for each detector. There are seasonal variations from about 290 K to 296 K over 15 years of Terra MODIS acquisitions for this band. The trending also reveals an explicit upward drift with a magnitude of 1.5 K. Figure 11 shows the detector-to-detector BT differences with respect to the scene average, calculated by averaging the BT over the detectors, before the crosstalk correction. The plot reveals that the differences for most detectors are between −0.5 K and +0.2 K with the exception of detectors 6 and 9.

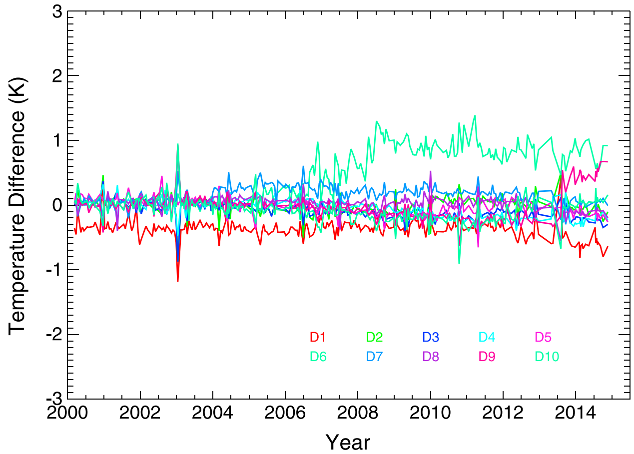

Figure 11. Terra MODIS band 29 C6 brightness temperature detector difference at Pacific Ocean, before correction.

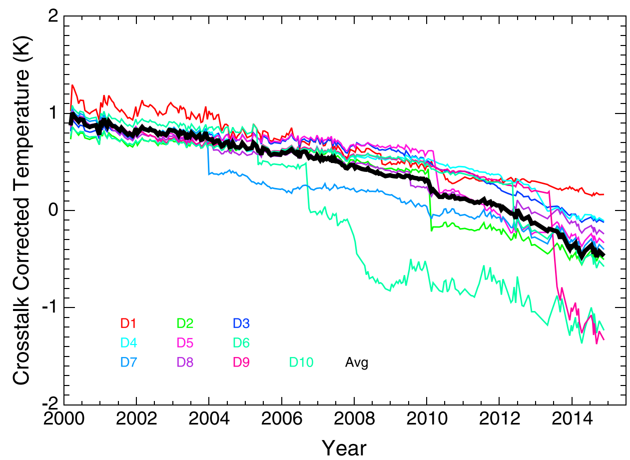

Figure 12. Crosstalk correction for Terra MODIS band 29 brightness temperature at Pacific Ocean.

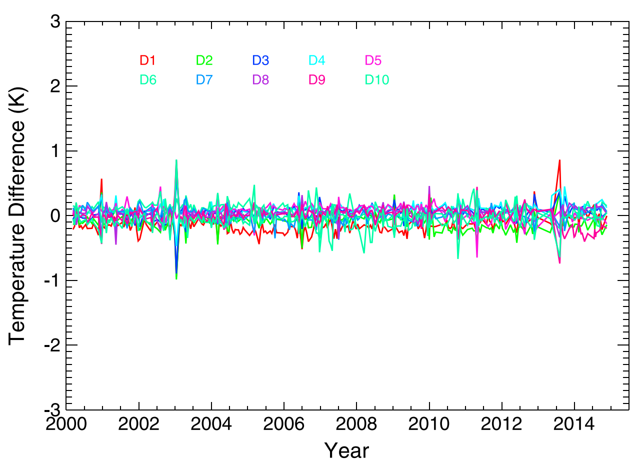

Figure 13. Terra MODIS band 29 C6 brightness temperature detector difference at Pacific Ocean after crosstalk correction.

Consistent with the b_1 trending before crosstalk correction, detectors 6 and 9 tend to have larger differences with respect to the scene average. The differences have tended to be small and within 0.6 K until 2006. Since 2006 the difference has increased and is about 1.5 K to this date. Thus, these detector-to-detector differences confirm the striping noise manifesting in band 29 imagery. Figure 12 gives the amount of crosstalk temperature correction based on the correction equation shown earlier. All detectors received a positive correction amount of close to 1 K in early life and a slightly lower negative crosstalk correction of about −0.3 K for most detectors in late life of the instrument operation. Detector 1 still receives a positive crosstalk correction today. Detectors 6 and 9 behaved in a normal fashion with the previous detectors before changing course since 2006 and 2014, respectively. They both have received the largest crosstalk correction amount of approximately −2.2 K. The thick black line in Figure 12 shows the band-averaged crosstalk correction for band 29, which was positive with a magnitude of 1 K early in the mission, gradually reduced, and became negative with a magnitude of −0.5 K recently. This indicates that the crosstalk effect induces a long-term upward drift of 1.5 K in Terra band 29 BT in the last 15 years. This is different from those observed in Terra bands 27 and 28, where the crosstalk effect induces downward long-term drifts of 6 K and 3 K, respectively. In other words, one may get opposite and different EV scene temperature trends from Terra bands 27–29. Figure 13 presents the detector-to-detector differences after the crosstalk correction is applied. The detector-to-detector differences are significantly reduced to be within ±0.2 K for all detectors. This consequentially would remove the striping artifacts in the crosstalk-corrected imagery for band 29. The band-averaged C6 BT before crosstalk correction and that after crosstalk correction over the ocean surface are presented in Figure 14 with dotted and solid lines, respectively. A long-term upward

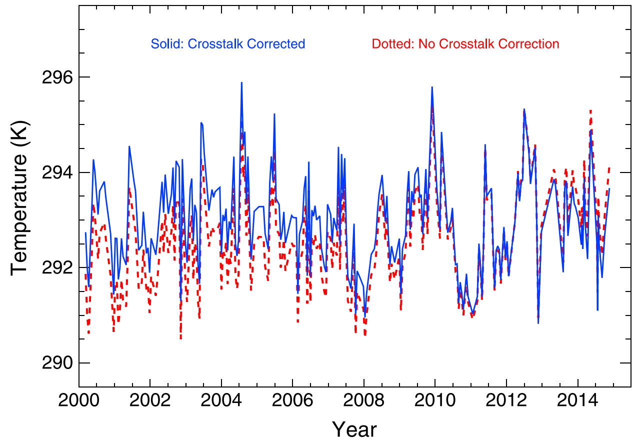

Figure 14. Band-averaged crosstalk correction with fitting for Terra MODIS band 28 at Libya 1.

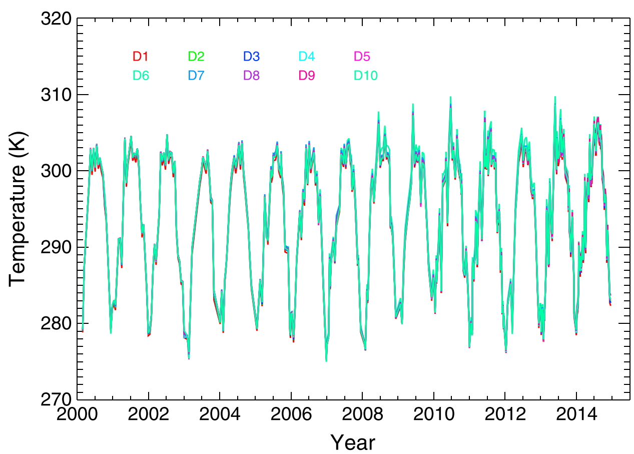

Figure 15. Terra MODIS band 29 C6 brightness temperature at Libya 1.

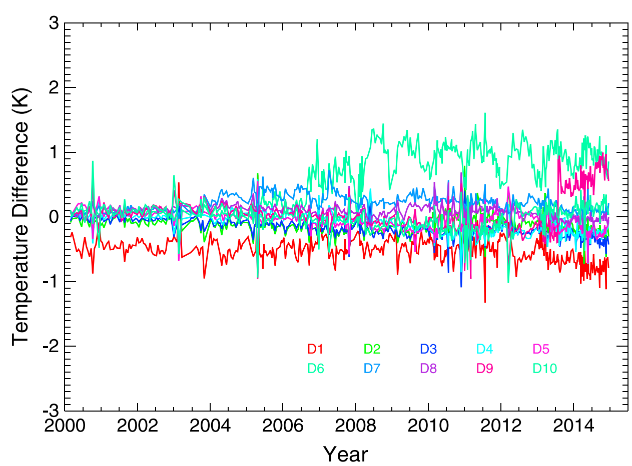

Figure 16. Terra MODIS band 29 C6 brightness temperature detector difference at Libya 1.

drift of 1.5 K is seen in dotted line and no noticeable long-term drift is observed in solid line. This indicates that the crosstalk correction significantly reduces the long-term drift. From various scientific studies reported in the Fifth Assessment Report (AR5), Intergovernmental Panel on Climate Change-28th Session, Budapest, Hungary, 9–10 April 2008 (http://www.ipcc.ch/report/ar5/index.shtml), it has been found that the sea surface temperatures over the Pacific Ocean have warmed by at least 1 K over a hundred year period from 1900. A +1.5 K drift over a 15 year period is deemed erroneous and is attributed to measurement deficiencies caused by the electronic crosstalk in Terra MODIS LWIR PV channels. For comparison of the crosstalk impact on EV BT among bands 27–29, the detector differences and the long-term drifts in 2012 are listed in columns 6 and 7 of Table 1, respectively. It is clearly seen from the table that the crosstalk effect in Terra band 29 is smaller than those in bands 27 and 28. It is worth to mention that the crosstalk effect induces a long-term upward drift in band 29 while a downward drift in the other two bands.

The Libya 1 desert site is geographically and radiometrically different in comparison to the Pacific Ocean site. In general, a desert site maintains higher daytime surface temperatures marked with cooler night temperatures. Also, the summer and winter temperature effects are fairly well pronounced when compared to ocean surfaces. Thus, the Libya 1 desert results analyze the temporal drifts at a slightly larger varying radiometric range. Figure 15 shows the long-term trending of BT responses for band 29 over the Libya 1 desert. The measured temperatures vary seasonally between 275 K and 300 K. A careful observation of the BT trends over Libya 1 also shows a small upward drift starting, especially from somewhere late 2008. As expected, the detector-to-detector differences from the scene average are quite varying and are shown in Figure 16. Detectors 2–5, 7–8, and 10 tended to have smaller differences on the order of approximately ±0.5 K. Detector 1 has a slightly larger bias of approximately 0.6 K and the difference is

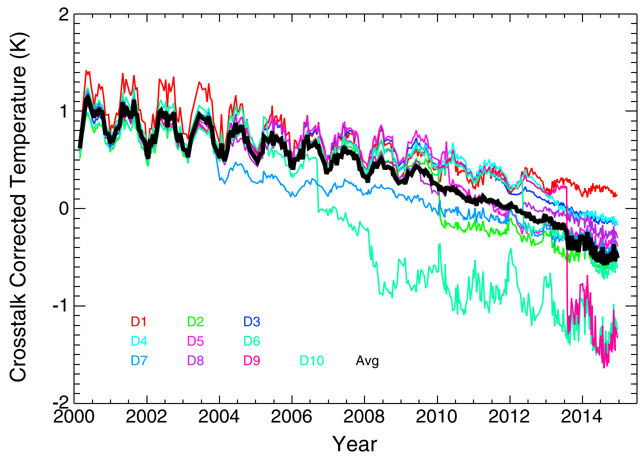

Figure 17. Crosstalk correction for Terra MODIS band 29 C6 brightness temperature at Libya 1.

about constant over lifetime. Detectors 6 and 9 trends in time are akin to that for the Pacific Ocean results. The differences have increased significantly from 2006 for detector 6 and from 2014 for detector 9. They are approximately 0.9 K at the end of 2014. Figure 17 gives the amount of crosstalk-corrected temperature for each of the detectors. The correction amounts are essentially similar to the Pacific Ocean site. All detectors tend to have a positive 1 K correction on average till mid-2004. A gradual linear decay in the correction amounts is assessed from 2004 onward. As of late 2014 the crosstalk correction amount is within ±0.6 K for all detectors except detectors 6 and 9. On average, detector 6 needs the largest crosstalk correction of approximately −1.0 K starting 2006, has continued to be fairly constant till 2012, and then continues to increase with a negative value. It is about −1.4 K currently. Detector 9 received positive crosstalk correction till late 2013 and then had a sudden change, dropping to a negative value of 1.2 K. Its current value is about 1.4 K, which is about the same as that of detector 6. The thick black line in Figure 17 is the band-averaged crosstalk correction, which shows a long-term downward drift. This indicates that the crosstalk effect induces a long-term upward drift in the BT of the band over the desert site, which is consistent with that over the Pacific Ocean site. Same as for Pacific Ocean site, the crosstalk correction is positive for the entire mission for detector 1. Figure 18 presents the detector-to-detector differences after crosstalk correction. The differences are significantly reduced in particular to the worst offending detectors 6 and 9 and are within ±0.3 K. As mentioned before, this would significantly alleviate the striping noise in the band 29 imagery. Figure 19 is similar to the trend shown in Figure 14. Long-term upward drift is noticeable in the dotted line, which is the band-averaged BT over Libya 1 before crosstalk correction. After the crosstalk correction, the drift definitely becomes smaller as shown in solid line. Since climate change may have larger impact on desert sites than on ocean sites, a noticeable surface temperature change on Libya 1 over 15 years is reasonable.

The study from both Pacific Ocean and Libya 1 confirms that the long-term drift induced by electronic crosstalk is systematic in nature when analyzed over the radiometric range of approximately 275 K–300 K. This sensing range indeed is a typical temperature range of band 29. Since the long-term drift at the Pacific Ocean site is about 1.5 K, the uncertainty of Terra band 29 C6 EV BT is at least 1.5 K, which is larger than 0.53 K, the uncertainty specification of the band [*Chiang et al.*, 2004]. After the crosstalk correction, the radiometric uncertainty of the band should be within the specification. Thus, with the crosstalk correction applied, the retrieved surface temperatures are then expected to keep in trend with the long-term climatic and environmental changes observed on a decadal time scale.

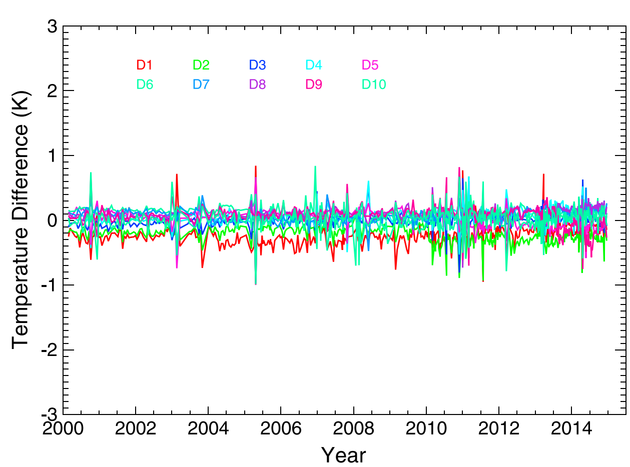

Figure 18. Terra MODIS band 28 C6 brightness temperature detector difference at Libya 1 after crosstalk correction.

It is worth to mention that for both of the selected sites, the signal level changes with season, especially the Libya 1 desert site, while our correction algorithm works for all seasons. The crosstalk effect is strongly detector dependent as demonstrated by the crosstalk coefficients and the detector difference before crosstalk effect correction. After the crosstalk correction is applied, the detector differences become much smaller and the

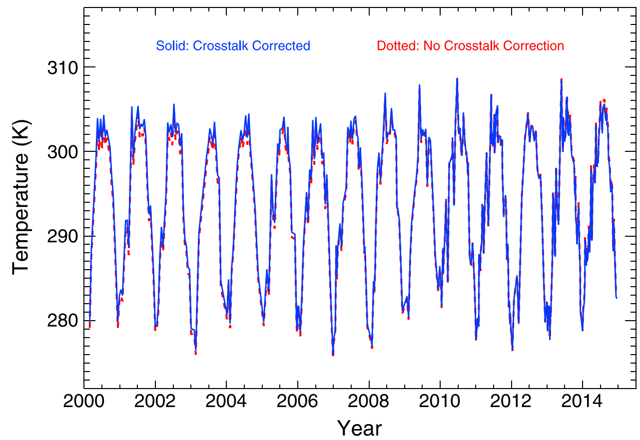

Figure 19. Band-averaged crosstalk correction with fitting for Terra MODIS band 28 at Libya 1.

differences almost time independent. This has also been demonstrated in Terra bands 27 and 28 [*Sun et al.*, 2014a, 2014b, 2015] as mentioned previously. In other words, the higher-order effect should be relatively small and, currently, no clear evidence shows that higher-order effects have significant contributions to the crosstalk effect.

5. Summary

The electronic crosstalk in the LWIR band 29 of Terra MODIS is established by analyses based on regularly scheduled lunar observations. The electronic crosstalk had severely affected detector 6 of band 29 rendering it to be classified as inoperable in the L1B quality assurance. A robust characterization of the crosstalk magnitude from the three sending bands 27, 28, and 30 allowed a good correction on two counts. First, the onboard BB calibration was improved. This was quantified by the improvements seen in the b_1 calibration term. The striping in the EV images is also significantly reduced due to detector differences that are greatly minimized. In particular, the detectors seemed to have equalized their gains which are certain to result in the removal of striping artifacts in the images. Further, the long-term drifts were assessed using two well-characterized radiometric sites. The Pacific Ocean site assessed the long-term drifts at typical BT levels of 300 K. The long-term drift was essentially removed with a very minor change on the order of about 0.02 K. Then, from the Libya 1 desert site the long-term drifts were assessed to be varying in a slow linear fashion after the crosstalk correction. While performing the analysis, scope for further considerations are identified. First, the first-order effects have been well understood, i.e., the effect of crosstalk on b_1, the dominant calibration term. Since most of the impact in MODIS TEB calibration is indeed absorbed by b_1 the offset and quadratic terms of the calibration play a second-order effect. Since the BB in MODIS is periodically operated at varying temperatures, it enables the offset and quadratic terms to be assessed. The effect of crosstalk on these minor calibration terms remains to be seen. Finally, a 1.5 K long-term drift in BT from band 29 is predicted based on the formality but it is a difficult one to be confirmed by the raw L1B products. This has to be confirmed via a different study such as one using ground target comparison.

Acknowledgments
The authors would like to thank Brij Gambhir and Mike Chu for their helpful comments and suggestions. The MODIS L1A data, which can be obtained at ftp://ladsweb.nascom.nasa.gov/allData/, are used in this analysis. The views, opinions, and findings contained in this paper are those of the authors and should not be construed as an official NOAA or U.S. Government position, policy, or decision.

References

Barnes, W. L., X. Xiong, and V. V. Salomonson (2002), Status of Terra MODIS and Aqua MODIS, *Proc. IGARSS*, *2*, 970–972.
Chiang, K., X. Xiong, A. Wu, and W. Barnes (2004), MODIS thermal emissive bands calibration uncertainty analysis, *Proc. of SPIE*, *5542*, 437–447.
Hook, S. J., W. R. Johnson, R. G. Radocinski, and G. Rivera (2014), In-flight validation of the mid and thermal infrared products from ASTER and MODIS on the Terra and Aqua platforms using the Lake Tahoe and Salton Sea automated validation sites, *Proc. SPIE*, *9218*, 9218–9229.
Li, W., X. Xiong, K. Chiang, and G. Toller (2005), Evaluation of Terra MODIS PC bands optical leak correction algorithm, *Proc. SPIE*, *5882*, 588219.
Madhavan, M., J. Sun, X. Xiong, B. N. Wenny, and A. Wu (2014), Statistical analysis of the electronic crosstalk correction in Terra MODIS Band 27, *Proc. SPIE*, *9218*, 9218–9275.
Salomonson, V. V., W. L. Barnes, X. Xiong, S. Kempler, and E. Masuoka (2002), An overview of the Earth Observing System MODIS instrument and associated data systems performance, *Proc. IGARSS*, *2*, 1174–1176.
Sun, J., and X. Xiong (2011), Solar and lunar observation planning for Earth-observing sensor, *Proc. SPIE*, *8176*, 817610.
Sun, J., X. Xiong, W. L. Barnes, and B. Guenther (2007), MODIS reflective solar bands on-orbit lunar calibration, *IEEE Trans. Geosci. Remote Sens.*, *43*, 2383–2393.
Sun, J., S. Madhavan, B. Wenny, and X. Xiong (2011), Terra MODIS band 27 electronic crosstalk: Cause, impact, and mitigation, *Proc. SPIE*, *8176*, 81760Z.
Sun, J., X. Xiong, S. Madhavan, and B. N. Wenny (2014a), Terra MODIS band 27 electronic crosstalk effect and its removal, *IEEE Trans. Geosci. Remote Sens.*, *52*, 1551–1561.
Sun, J., X. Xiong, Y. Li, S. Madhavan, A. Wu, and B. N. Wenny (2014b), Evaluation of radiometric improvements with electronic crosstalk correction for Terra MODIS band 27, *IEEE Trans. Geosci. Remote Sens.*, *52*, 6497–6507.
Sun, J., S. Madhavan, X. Xiong, and M. Wang (2014c), Electronic crosstalk correction for Terra long wave infrared photovoltaic bands, *Proc. SPIE*, *9264*, 926412.
Sun, J., S. Madhavan, X. Xiong, and M. Wang (2015), Investigation of the electronic crosstalk in Terra MODIS band 28, *IEEE Trans. Geosci. Remote Sens.*, *53*, 5722–5733.

Wenny, B. N., A. Wu, S. Madhavan, Z. Wang, Y. Li, N. Chen, V. Chiang, and X. Xiong (2012), MODIS TEB calibration approach in collection 6, *Proc. SPIE*, *8533*, 85331 M.

Wenny, B. N., X. Xiong, S. Madhavan, A. Wu, and Y. Li (2013), Long-term band-to-band calibration stability of MODIS thermal emissive bands, *Proc. SPIE*, *8724*, 872412.

Xiong, X., N. Che, and W. Barnes (2006), Terra MODIS on-orbit spectral characterization and performance, *IEEE Trans. Geosci. Remote Sens.*, *44*(8), 2198–2206.

Xiong, X., J. Sun, W. Barnes, V. V. Salomonson, J. Esposito, H. Erives, and B. Guenther (2007), Multi-year on-orbit calibration and performance of Terra MODIS reflective solar bands, *IEEE Trans. Geosci. Remote Sens.*, *45*, 879–889.

Xiong, X., K. Chiang, A. Wu, W. Barnes, B. Guenther, and V. Salomonson (2008), Multiyear on-orbit calibration and performance of Terra MODIS thermal emissive bands, *IEEE Trans. Geosci. Remote Sens.*, *46*, 1790–1803.

Xiong, X., B. Wenny, A. Wu, and W. Barnes (2009), MODIS on-board blackbody function and performance, *IEEE Trans. Geosci. Remote Sens.*, *47*.

Xiong, X., A. Wu, B. N. Wenny, S. Madhavan, Z. Wang, Y. Li, N. Chen, W. Barnes, and V. Salomonson (2015), Terra and Aqua MODIS thermal emissive bands on-orbit calibration and performance, *IEEE Trans. Geosci. Remote Sens.*, *53*, 5709–5721.